Comparative studies of etching mechanisms of CR-39 in NaOH/H$_2$O and NaOH/ethanol

K.C.C. Tse, D. Nikezic, K.N. Yu *

Department of Physics and Materials Science, City University of Hong Kong, Tat Chee Avenue, Kowloon Tong, Hong Kong

Available online 13 May 2007

Abstract

The bulk etch rate for CR-39 in NaOH/ethanol was faster than those in aqueous solution of NaOH (NaOH/H$_2$O). Furthermore, a layer of precipitate always accumulates on the surface of CR-39 detector during etching in NaOH/ethanol, which is absent during etching in NaOH/H$_2$O. In the present work, mass spectrometry results have shown that the same etched products are present in the etchants of NaOH/H$_2$O and NaOH/ethanol after etching of CR-39. This shows that CR-39 has the same etching mechanism in both etchants. These etched products support the etching mechanism of scission of the carbonate ester bond in CR-39 by the hydroxide ion through basic hydrolysis of ester. The difference in the bulk etch rates can be explained in terms of the solubility of the etched products in the etchants. FTIR analyses of the solute formed from the etchants show the formation of allyl alcohol and carbonate during etching in both etchants. The FTIR spectra of the precipitate formed at the surface of CR-39 detectors during etching in NaOH/ethanol has also shown that sodium carbonate is present in the precipitate. Finally, XRD analyses of the solute formed from the etchants show the formation of sodium bicarbonate and sodium carbonate in the etchant of NaOH/H$_2$O after etching and the formation of the mineral natrite and thermonatrite in the etchant of NaOH/ethanol as well as in the layer of precipitate on the surface of the CR-39 detector formed during etching in NaOH/ethanol.
© 2007 Elsevier B.V. All rights reserved.

PACS: 29.40; 23.60

Keywords: Solid-state nuclear track detector; SSNTD; CR-39; Etching mechanism

1. Introduction

The CR-39 detector (poly(diethyleneglycol bis[allylcarbonate])) is a commonly used solid-state nuclear track detector (SSNTD). A recent review of SSNTDs can be found in ref. [1]. The bulk etch rates V_b for CR-39 were found to be much faster in NaOH/ethanol than those in aqueous solution of NaOH (NaOH/H$_2$O) [2,3]. For example, the bulk etch rates for CR-39 in 0.5 M NaOH/ethanol at 55 °C and 6.25 M NaOH/H$_2$O at 70 °C were found to be 22 and 1.2 μm/h, respectively, [3,4]. Therefore, it is pertinent to study and understand the reasons behind the very different bulk etch rates V_b. This forms the first objective of the present paper. Moreover, it has been observed that a layer of

precipitate always accumulates on the surface of CR-39 detector during its etching in NaOH/ethanol, which is absent during its etching in NaOH/H$_2$O. It is thus also important to study the nature as well as the formation mechanism of this precipitate. For example this has implications for procedures for fast and even etching of CR-39 detectors using NaOH/ethanol as the etchant [5]. The study of the precipitate forms the second objective of the present paper.

The etching mechanisms of CR-39 detectors in NaOH/H$_2$O and NaOH/ethanol were studied through mass spectrometry studies of the etchants after etching the detectors. Fourier transform infrared (FTIR) spectroscopy of the detectors themselves as well as the solutes formed from the etchants after etching and also X-ray diffractometer (XRD) studies of the solutes formed from the etchants after etching was carried out. The layer of precipitate formed at the surface of CR-39 detectors during etching in NaOH/ethanol was also studied using FTIR and XRD.

---

* Corresponding author. Tel.: + 852 27887812; fax: + 852 27887830.
 E-mail address: peter.yu@cityu.edu.hk (K.N. Yu).

2. Methodology

2.1. CR-39 detectors and etching

For the present work, the CR-39 detectors were purchased from Page Mouldings (Pershore) Limited (Worcestershire, UK). The molecular structure of the CR-39 monomer is shown in Fig. 1. Two types of CR-39 detectors were purchased and employed in the present studies, namely, those with thickness of 1000 and 100 μm. The CR-39 samples with thickness between 30 and 100 μm were obtained by etching the 100 μm CR-39 detectors in 0.5 M NaOH/ethanol in our laboratory.

The etch products of CR-39 were studied to provide information on the etching mechanisms of CR-39 in NaOH/H_2O and NaOH/ethanol. CR-39 detectors with dimensions $3 \times 3 \times 0.1$ cm^3 were etched in 6.25 M NaOH/H_2O at 70 °C and 0.5 M NaOH/ethanol at 55 °C, respectively, for 6 h. The temperature was kept constant with an accuracy of ±1 °C. Etching of CR-39 in NaOH/ethanol was carried out in a sealed environment to prevent the evaporation of ethanol.

2.2. Mass spectrometry

The liquid-chromatography–mass spectrometry (LC–MS) system (PE/SCIEX API 365) was employed to identify the etched products in the etchants of NaOH/H_2O and NaOH/ethanol by analysis of the mass/charge ratio m/z given in the mass spectra for both positive and negative ions.

2.3. FTIR spectroscopy

The FTIR spectroscopy system employed for the present work was the Perkin Elmer Model 16 PC FTIR system. The FTIR spectrometer can be operated in the transmission mode or the specular reflection mode. Transmission mode was employed for the present experiments. The absorption bands originate from the interaction of the electrical vector of the electromagnetic wave with the electrical dipole of non-symmetrical bonds. In other words, if the dipole corresponding to a chemical bond oscillates at the same frequency of the electromagnetic wave, the electrical component of the wave can transfer its energy to the bond. Some of the absorption bands are identified with the help of Software Spectrum Search Plus (ver. 2.0, Perkin Elmer).

The working wave number range of the spectrometer was from 4000 to 400 cm^{-1}, with a resolution of 4 cm^{-1}. FTIR spectra of the thin CR-39 detectors were first examined to study all the absorption bands related to the polymer chain. The thick CR-39 detector cannot be used for this purpose since it is too thick and the infrared radiation at some wave numbers will be entirely absorbed. Each CR-39 detector was scanned for 30 cycles to obtain the spectrum, which plotted the transmittance as a function of the wave number.

After etching, depending on the objective, either a portion of the etchant or the layer of precipitate formed at the surface of CR-39 detectors during etching in NaOH/ethanol was dried in an oven at 60 °C and the remaining solid sample was crushed together with dry KBr (2% mass ratio) in a mortar. The mixture was compressed into a disc using a hydraulic press with a pressure of 10 ton/cm^2. The disc samples were then analyzed by FTIR.
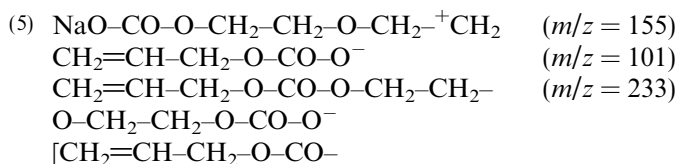
2.4. X-ray diffraction

After etching of CR-39 in NaOH/H_2O and NaOH/ethanol, the etchants were dried in an oven. The solutes formed from the etchants were separately ground to fine powders before being mounted in the sample chamber for irradiation with collimated X-rays. XRD with Cu Kα radiation, whose characteristic wavelength was 1.54056 Å, was performed using the Siemens D500 Powder Diffractometer operated in coupled scanning. The step time and the step size were 1 s and 0.020°, respectively. The detection range of 2θ was between 20° and 80°. XRD spectra of the solutes were obtained and the etched products were confirmed by checking the strongest diffraction lines with the literature using the software PCPDFIN ver. 1.20 (International Centre for Diffraction Data® (ICDD®)).
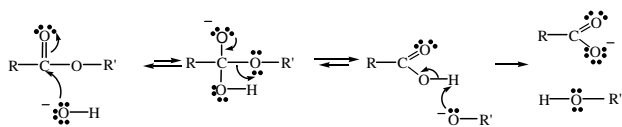
3. Results and discussion

3.1. Results from mass spectrometry

In both the etchants of NaOH/H_2O and NaOH/ethanol, our mass spectrometry results have identified the following radicals/ions (with the m/z ratios shown), which indicate creation of the species shown in square brackets below during etching of CR-39:
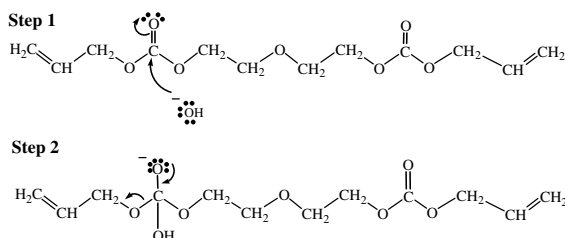
(1) HO–CH_2–CH_2–O–CH_2 –CH=$^+$OH   ($m/z = 105$)
HO–CH_2–CH_2–O–CH_2 –CH_2–O$^-$ ($m/z = 105$)
[2,2-oxydiethanol: HO–CH_2–CH_2–O–CH_2–CH_2–OH]

(2) CH_2=CH–CH_2–O– CO–O$^-$ ($m/z = 101$)
[2-propenyl carbonate: CH_2=CH–CH_2–O–CO–ONa]

(3) HO–CH_2–CH_2–O$^-$ ($m/z = 61$)
CH_2=CH–CH_2–O–CO–O–CH_2–$^+CH_2$ ($m/z = 129$)
[CH_2=CH–CH_2–O–CO–O–CH_2–CH_2–O–CH_2–CH_2–OH]

(4) NaO–CO–O–CH_2–CH_2–O–CH_2–CH=$^+$OH   ($m/z = 171$)
NaO–CO–O–CH_2–CH_2–O–CH_2–CH_2–O$^-$ ($m/z = 171$)
[NaO–CO–O–CH_2–CH_2–O–CH_2–CH_2–OH]

(5) NaO–CO–O–CH$_2$–CH$_2$–O–CH$_2$–$^+$CH$_2$ (m/z = 155)
CH$_2$=CH–CH$_2$–O–CO–O$^-$ (m/z = 101)
CH$_2$=CH–CH$_2$–O–CO–O–CH$_2$–CH$_2$– (m/z = 233)
O–CH$_2$–CH$_2$–O–CO–O$^-$
[CH$_2$=CH–CH$_2$–O–CO–

It is very interesting to observe that the same etched products are present in both the etchants of NaOH/H$_2$O and NaOH/ethanol. This shows that in fact CR-39 has the same etching mechanism in both etchants. These etched products support the etching mechanism of scission of the carbonate ester bond in CR-39 by the hydroxide ion through basic hydrolysis of ester [6,7]. CR-39 detectors (see the monomer structure in Fig. 1) contain the functional group of ester. Under the basic hydrolysis of ester, the hydroxide ion causes the scission of the ester linkage:
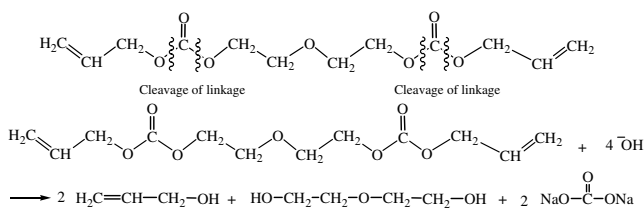

or in short, R–CO–OR$'$ + OH$^-$ → R–CO–O$^-$ + R$'$–OH. In the context of CR-39, therefore, the mechanism of attacking the carbon atom of the alkoxycarbonyl group by the hydroxide ion is as follows:
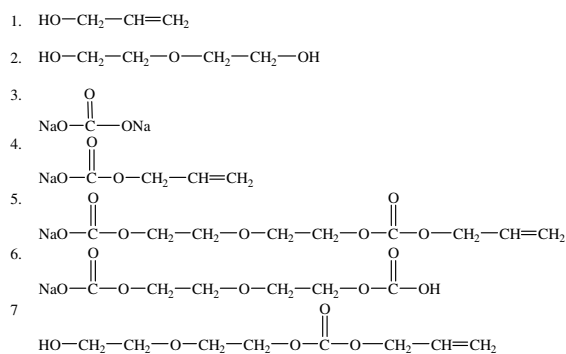

In fact, there are four possible positions which are subjected to cleavage by the hydroxide ion:

Reaction showing the position of cleavage of linkage by hydroxide ion OH$^-$:

In the hydrolysis of ester in the CR-39 monomer, the hydroxide ions will attack the carbon atom of the alkoxycarbonyl group to produce 2-propen-1-ol/allyl alcohol

CH$_2$=CHCH$_2$OH, 2,2-oxydiethanol HOCH$_2$CH$_2$OCH$_2$CH$_2$OH and sodium carbonate Na$_2$CO$_3$ [6]. A variety of etched products can be produced due to cleavages of the linkage of carboalkoxy group –CO–O– at different positions. Possible etched products are:

The etched products 2, 4, 5, 6 and 7 are clearly identified in our mass spectrometry results. Product 1 was not observed since we did not analyze the spectrum down to such a small molecular mass and there are a number of species identified in the mass spectrometry results which point to the formation of product 3.

Now that CR-39 has the same etching mechanism in both the etchants of NaOH/H$_2$O and NaOH/ethanol, the difference in the bulk etch rates can be explained in terms of the solubility of the etched products in the different etchants. It is well established that polar compounds are highly soluble in other polar compounds but virtually insoluble in nonpolar compounds. Therefore, the etched products from CR-39 are more soluble in ethanol, which explains the enhancement of the bulk etch rates in the etchant of NaOH/ethanol.

3.2. Results from FTIR spectroscopy

The FTIR spectra of CR-39 detectors with different thickness, namely, 30, 140, 180 and 1048 μm, are shown in Fig. 2. The absorption peaks corresponding to O–H stretching vibration (3636 and 3549 cm^{-1}) [8], C=O stretching vibration (3473, 1766, 1264 and 1141 cm^{-1}), C–O–C stretching vibration (1096 and 1026 cm^{-1}), –CH=CH$_2$ stretching vibration (3074 and 1650 cm^{-1}), C=C deformation vibration (964 cm^{-1}), C–H stretching vibration (2952 cm^{-1}) [9], C–H deformation vibration (1456, 1405, 879 and 788 cm^{-1}) decreased when the thickness of the CR-39 detector decreases, so these peaks are characteristic of the CR-39 detector. The peaks at 3635 and 3550 cm^{-1} were assigned to the OH anti-symmetric stretching and O–H symmetric stretching, respectively. The peak at 3473 cm^{-1} was the overtone of C=O stretching vibration of ester. The wave numbers corresponding to these absorptions (transmission troughs) and the
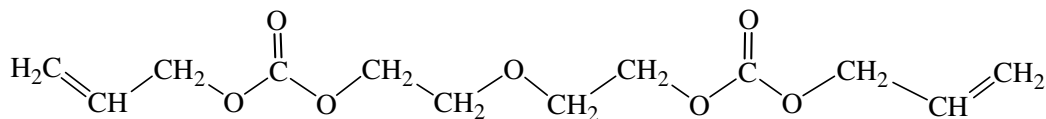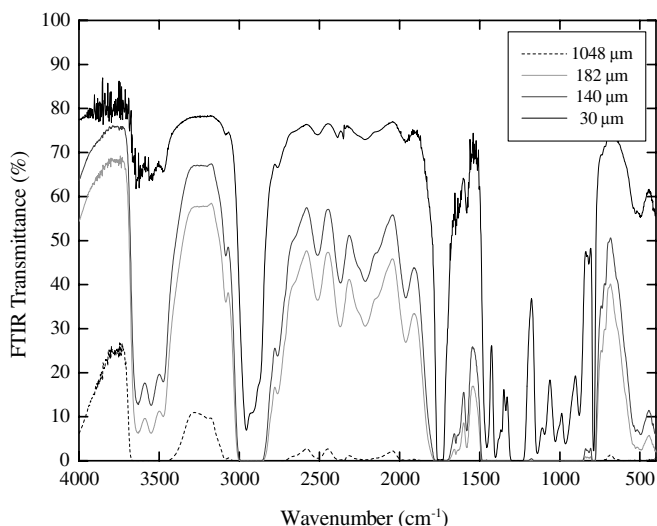
Fig. 1. Structure of the CR-39 monomer.

Fig. 2. FTIR spectra in the transmission mode for CR-39 detectors with different thickness, viz. 30, 140, 182 and 1048 μm, with a linear scale abscissa in cm^{-1} and % transmittance as the ordinate.

Table 1
The wave numbers of the more significant absorption peaks (transmission troughs) in the FTIR spectrum of CR-39 and the corresponding assignment of the function groups and the modes of vibration

Position of the peak (cm^{-1})	Function group/modes of vibration
3636	OH anti-symmetric stretching
3549	OH symmetric stretching
3473	First overtone of C=O stretching vibration of ester
3074	=CH alkenes stretching vibration
2952	Asymmetric CH$_2$ stretching vibrations for aliphatic hydrocarbons
2912	Symmetric CH$_2$ stretching vibrations for aliphatic hydrocarbons
1766	Ester C=O stretching vibration of alkyl carbonates –O–CO–O–
1650	Hydrocarbons C=C stretching of vinyl group (–CH=CH$_2$)
1456	CH$_2$ and CH$_3$ deformation vibration –OCH$_2$ deformation vibration of –CO–O–CH$_2$
1402	CH$_3$ symmetric deformation vibration OCH$_2$ wagging vibration of –CO–O–CH$_2$
1264	Asymmetric stretching vibration of C–O–C of aliphatic ester
1141	Symmetric stretching vibration of C–O–C group for aliphatic ester
1096	Asymmetric stretching vibration of C–O–C group for saturated aliphatic ether
1026	Symmetric stretching vibration of C–O–C group for saturated aliphatic ether
964	Wagging vibration of the double bond C=C
879	CH rocking out of plane deformation
788	CH rocking out of plane deformation

corresponding assignment of the functional groups and the modes of vibration are shown in Table 1.

On the other hand, the FTIR spectra of the solute disc formed from the etchant are shown in Fig. 3. The alkene C=C stretching vibration and the O–H stretching vibration were observed at 1642 and 3412 cm^{-1}, respectively, which may suggest the formation of allyl alcohol. The presence of the absorption band at 1422, 1068, 864 and 686 cm^{-1} suggested the presence of the carbonate. The broad absorption band near 3400 cm^{-1} corresponding to the OH of water of crystallization suggested that the etched product was a hydrated carbonate. With the help of the Spectrum Search Plus software, we have identified that sodium carbonate (Na$_2$CO$_3$) was formed in the reactions for both etchants of NaOH/H$_2$O and NaOH/ethanol.

Finally, the FTIR spectra for the precipitate formed at the surface of CR-39 detectors during etching in NaOH/ethanol has also shown that sodium carbonate is present in the precipitate. Sodium carbonate is the disodium salt of carbonic acid. It is a gray-white powder that is soluble in water but not in organic solvents. Comparing the bulk etch rates of CR-39 detector in NaOH/H$_2$O and NaOH/ethanol, the production rate of sodium carbonate in the latter one was larger. Due to the insolubility of sodium carbonate and its saturation in ethanol, a layer of precipitate was accumulated on the surface of CR-39, which was absent when the etchant NaOH/H$_2$O was used.

3.3. Results from XRD analysis

By comparing the strongest lines in the XRD spectra with the literature, the crystalline products in the solutes from the etchants were identified [10]. The XRD spectra of the solutes from the etchants NaOH/H$_2$O and NaOH/ethanol are shown in Fig. 4. Sodium bicarbonate (NaHCO$_3$), which was represented by the diffraction lines 2.95, 2.59, 2.19, 2.03 and 3.22 Å and sodium carbonate (Na$_2$CO$_3$), which was represented by the diffraction lines 2.36, 2.96, 2.59, 2.54 and 2.18 Å, were formed in the etchant of NaOH/H$_2$O after etching of CR-39. For both the etchant of NaOH/ethanol and the layer of precipitate on the surface of the CR-39 detector, formation of the mineral Natrite Na$_2$CO$_3$ was represented by the strongest lines 2.96, 2.37, 2.55, 2.60 and 2.62 Å while formation of Thermonatrite Na$_2$CO$_3$ · H$_2$O was represented by the strongest lines 2.76, 2.37, 2.68, 2.47 and 2.24 Å.
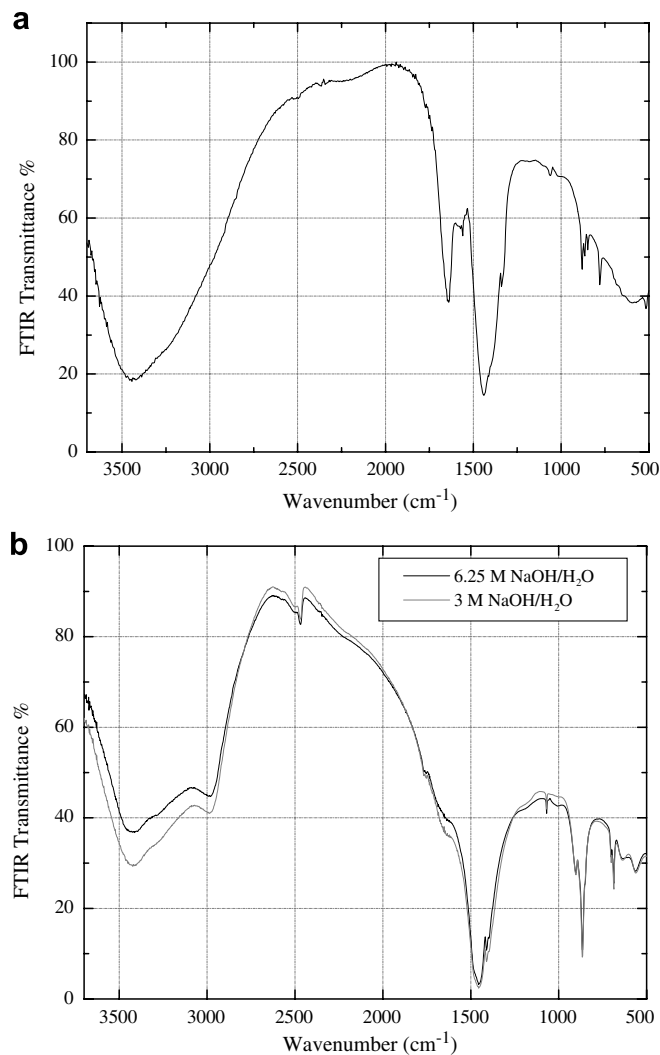
Fig. 3. (a) FTIR spectrum in transmission mode of the etchant of 0.5 M NaOH/ethanol after the reaction with CR-39 at 55 °C. (b) FTIR spectra in the transmission mode of the etchant of 3 M and 6.25 M NaOH/H$_2$O after the reaction with CR-39 at 70 °C.

Fig. 4. XRD spectrum of solutes from the etchants: (a) 0.5 M NaOH/ethanol at 55 °C for etching time of 6 h; (b) 6.25 M NaOH/H$_2$O at 70 °C for etching time of 55 h. The peak numbers represent the diffraction spacing *d*.

4. Conclusions

(1) The mass spectrometry results have shown that the same etched products are present in the etchants of NaOH/H$_2$O and NaOH/ethanol after etching of CR-39. This shows that in fact CR-39 has the same etching mechanism in both etchants. These etched products support the etching mechanism of scission of the carbonate ester bond in CR-39 by the hydroxide ion through basic hydrolysis of ester. The difference in the bulk etch rates can then be explained in terms of the solubility of the etched products in the etchants. The etched products are more soluble in ethanol, which explains the enhancement of the bulk etch rates of CR-39 in NaOH/ethanol.

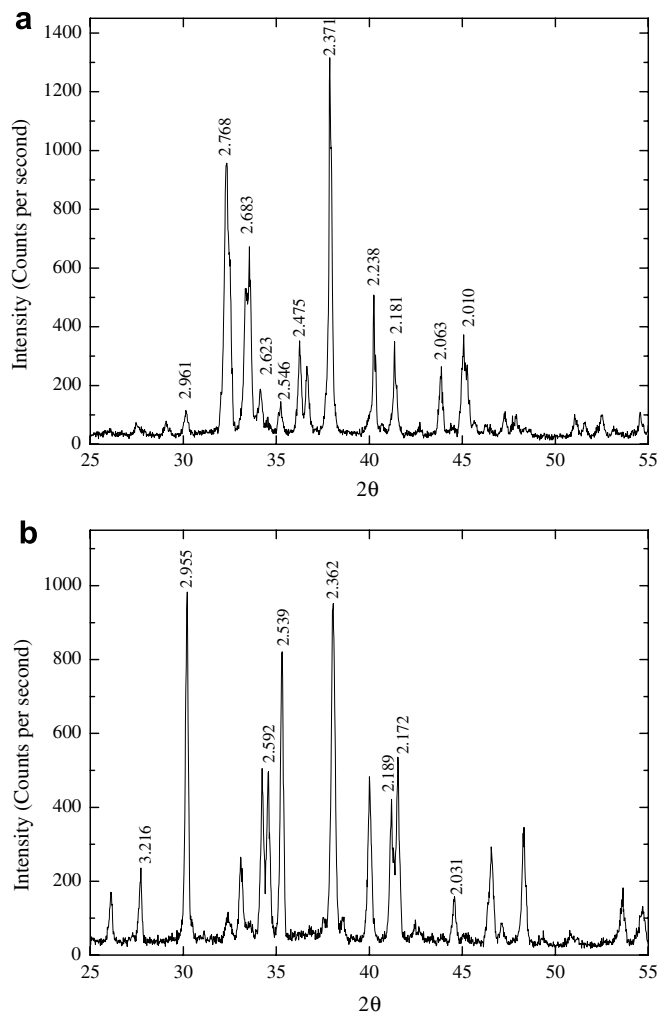(2) The FTIR analyses of the solute formed from the etchants show the formation of allyl alcohol and carbonate during etching of CR-39 in both etchants of NaOH/H$_2$O and NaOH/ethanol. The FTIR spectra of the precipitate formed at the surface of CR-39 detectors during etching in NaOH/ethanol has also shown that sodium carbonate is present in the precipitate. Due to the insolubility of sodium carbonate and its saturation in ethanol, a layer of precipitate was accumulated on the surface of CR-39, which was absent when the etchant NaOH/H$_2$O was used.

(3) The XRD analyses of the solute formed from the etchants show the formation of sodium bicarbonate (NaHCO$_3$) and sodium carbonate (Na$_2$CO$_3$) in the etchant of NaOH/H$_2$O after etching of CR-39 and the formation of the mineral Natrite Na$_2$CO$_3$ and Thermonatrite Na$_2$CO$_3 \cdot$ H$_2$O in the etchant of NaOH/ethanol as well as in the layer of precipitate on the surface of the CR-39 detector formed during etching of CR-39 in NaOH/ethanol.

Acknowledgement

References

[1] D. Nikezic, K.N. Yu, Mater. Sci. Eng. R 46 (2004) 51.
[2] Matiullah, S. Rehman, S. Rehman, W. Zaman, Radiat. Meas. 39 (2005) 337.
[3] K.F. Chan, F.M.F. Ng, D. Nikezic, K.N. Yu, in: 6th International Topical Meeting on Industrial Radiation and Radioisotope Measurement Applications, 20–24 June, 2005, McMaster University, Canada, paper 110.
[4] J.P.Y. Ho, C.W.Y. Yip, D. Nikezic, K.N. Yu, Radiat. Meas. 36 (2003) 141.
[5] K.F. Chan, B.M.F. Lau, D. Nikezic, A.K.W. Tse, W.F. Fong, K.N. Yu, in: 6th International Topical Meeting on Industrial Radiation and Radioisotope Measurement Applications, 20–24 June, 2005, McMaster University, Canada, paper 111.
[6] T.A. Gruhn, W.K. Li, E.V. Benton, R.M. Cassou, C.S. Johnson, in: 10th International Conference on Solid State Nuclear Track Detectors, 1979, p. 291.
[7] X.T. Nguyen, T.D. Trinh, Radiat. Meas. 25 (1995) 185.
[8] M.A. Malek, C.S. Chong, Vib. Spectrosc. 24 (2000) 181.
[9] S. Gaillard, V. Armbruster, M.A. Hill, T. Gharbi, M. Fromm, Radiat. Res. 163 (2005) 343.
[10] S.N. Husaini, N.U. Khattak, A.A. Qureshu, F. Malik, I.E. Qureshi, T. Karim, H.A. Khan, Radiat. Meas. 35 (2002) 3.